Chapter 6

Constraining Dark energy equation of state using the 21-cm and Ly-α forest cross correlation

6.1 Introduction

Over the last decade a large number of precise cosmological observations have indicated that the Universe is in an accelerated expansion [1, 275]. The underlying cause of the cosmic acceleration in the the later part of the matter dominated epoch is, however, still an unresolved question. In the standard cosmological paradigm the cosmic acceleration is explained by a dark energy component as a new kind of fluid with an equation of state (EoS) $p/\rho = w(< -1/3)$. Several probes of cosmology have made precise measurements of cosmological parameters which now indicates that bulk of the matter/energy budget of the Universe (approximately $\sim 70\%$) has the energy density in the form of dark energy [276–279] and the remaining $\sim 30\%$ in the form of non-relativistic matter comprising of both baryonic matter and dark matter. We have also seen that dark matter is classified into a cold, warm and hot dark matter categories. In this chapter we shall focus on dark energy. Einstein's general theory of relativity gives us a natural candidate for constant dark energy as the cosmological constant Λ. If we assume that the cosmological constant is non-zero, then it may be seen as a fluid. In this model of the cosmological constant as "dark energy" the equation of state is simple and is given by $w = -1$. This model is tested by many precision observations. For consistency with quantum field theory and particle physics the cosmological constant Λ is interpreted as a non-zero vacuum energy density [280]. There are theoretical

difficulties with the cosmological constant, the most serious being the the 'fine tuning' problem. Further, in recent times observational data on low redshift measurements of H_0 [4] also have found tension with the commonly accepted CMBR projections from Planck-2015 that predicts a flat $LCDM$ model. The understanding of dark energy is far from complete. Apart from theoretical difficulties there a strong indications that instead of a constant Λ, a dynamical dark energy model maybe preferable over the concordance $LCDM$ model [5] with high statistical significance. These observations point towards gaps in our true understanding of dark energy.

Many dynamic Dark energy models have been proposed as an alternative to the cosmological constant. These models often involves a scalar field [281–293]. The dynamics of these scalar fields with suitable intial conditions is used to explain the phenomenology of cosmic acceleration. Given the immense diversity of proposed scalar field models, it generally difficult to constrain them from observational data. However, it becomes more convenient if these models can be described by some general parametrizations which reproduce their general behaviour for the expansion history. The most common form of this parametrization involved the EoS. In this parametrization the ratio $p/\rho = w(z)$ is made redshift dependent to invoke evolution of dark energy [288, 294–297]. It has also been shown that a 2-parameter description is optimal for $w(z)$. The parametrization of the EoS given by Chavallier-Linder-Polarski (henceforth CPL), [297, 298] is one of the most popularly used 2-parameter model for dark energy. We shall also consider two commonly used variant of the CPL model called the Barboza-Alcaniz (BA) model [299].

6.2 Dark energy models

The Friedmann equation for the evolution of the Hubble parameter $H(a)$ in a spatially flat ($\Omega_K = 0$) FRW Universe is given by

$$\frac{H(a)}{H_0} = \sqrt{\Omega_{m_0} a^{-3} + (1 - \Omega_{m_0}) \exp\left[-3 \int_1^a da' \frac{1 + w(a')}{a'}\right]} \tag{6.1}$$

where H_0 and Ω_{m_0} denote the present $z = 0$ values of the Hubble parameter and the matter density parameter respectively. The dark energy component is assumed to be modeled with an evolving EoS $w(a)$, and the matter budget also consists dark matter and baryonic matter. We have used the cosmological parameters Planck18

results

$$(\Omega_{m_0}, \Omega_{b_0}, H_0, n_s, \sigma_8, \Omega_K) = (0.315,\ 0.0496,\ 67.4,\ 0.965,\ 0.811,\ 0)$$

from [300] throughout this work.

While this gives the background evolution of the scale factor the equation governing the growth of perturbations is given by the equation for the growing mode

$$\frac{d^2 D_+}{d(\ln a)^2} + \frac{1}{2}\left(1 - 3w(z)\Omega'(z)\right)\frac{dD_+}{d\ln a} - \frac{3}{2}\Omega_m(z)D_+ = 0 \tag{6.2}$$

where $\Omega'(z) = 1 - \Omega_m(z)$. The growth rate of density perturbations $f = \frac{d\ln D_+}{d\ln a}$ is a quantifier of structure formation. Figure (6.1) shows the variation of f with redshift for different CPL parametrizations. The departure from the LCDM model is of the order of a few percent. Figure (6.2) shows the variation of f for different BA parametrizations. The generic behaviour is same as the CPL model and a few percent departure from the LCDM is seen.

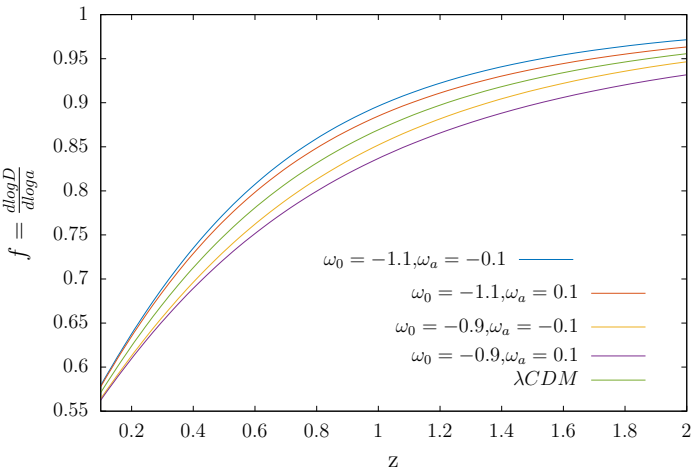

Figure 6.1: The growth rate of density perturbations for different CPL parametrizations.

We recognize easily that if the dynamics of Dark energy is modelled using the EoS parametrization $w(z)$ with $a = 1/(1+z)$, a wide variety of possible choices for $w(z)$ shall be possible. Though such a diversity of parametrization exist, it has been shown that from the observational perspective at most a two-parameter model can be best constrained [301]. These parametrizations are phenomenological and are model-free. The model proposed by Chevallier Polarski [297] and Linder

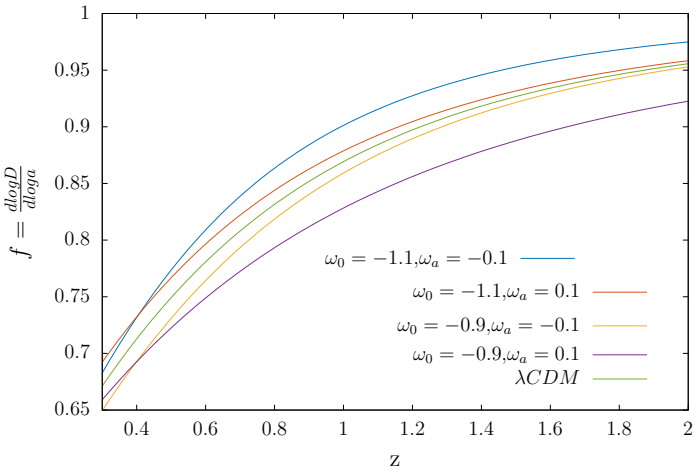

Figure 6.2: The growth rate of density perturbations for BA parametrizations

[298] and a wide class of quintessence scalar field models are describable by the CPL parametrization [302]. However a better fit to both tracking and thawing class of models require a generalization of the CPL parametrization [303].

We use the following parametrizations in this work

$$w_{_{CPL}}(z) = w_0^{CPL} + w_a^{CPL}\left(\tfrac{z}{1+z}\right) \qquad (CPL) \tag{6.3}$$

$$w_{_{BA}}(z) = w_0^{BA} + w_a^{BA}\left(\tfrac{z(1+z)}{1+z^2}\right) \qquad (BA) \tag{6.4}$$

Each model is characterized by two constant parameters (w_0, w_a) with w_a quantifying the evolution of dark energy from its present value set by w_0.

Density fluctuations drive acoustic waves in the primordial baryon-photon plasma. These sound waves are frozen once recombination takes place at $z \sim 1000$. This leaves a distinct oscillatory signature on the CMBR temperature power spectrum [304]. Thus, the sound horizon at the epoch of recombination becomes a standard ruler against which cosmological distances are to be calibrated. Since $\sim 15\%$ of the total matter density is in the form of baryons, this oscillatory feature known as the baryon acoustic oscillations are also imprinted in the low redshift matter power spectrum. The oscillatory feature on CMBR temperature power spectrum is an order unity effect, however at low redshifts, the signal gets suppressed by a factor $\sim \Omega_b/\Omega_m \sim 0.1$ [305]. The baryon acoustic oscillation (BAO) is a potentially powerful cosmological probe [306, 307]. This effect occurs on large scales ($\sim 150\,\mathrm{Mpc}$), where the fluctuations are can be still analysed using a linear theory. BAO observations allow us to measure the angular diameter distance $D_A(z)$ and the Hubble parameter $H(z)$ as functions of redshift using the imprint of the os-

cillatory feature in the transverse and the longitudinal directions respectively and thereby allows us to constraint on dark energy models. Projections for detecting the BAO signal using redshift 21-cm emission has been reported [308–310]. BAO has also been precisely measured at $z \sim 0.57$ using the galaxies in the SDSS III Baryon Oscillation Spectroscopic Survey (BOSS; [311]). Detecting the BAO signal in the Lyman-α forest has been forecasted [141]. The BAO signal has also been detected at $z \sim 2.3$ [312] using the BOSS Lyman-α forest data. The combination $D_A^{0.2}\, H^{-0.8}$ has been measured at a 3.5% level. Using results for the BOSS

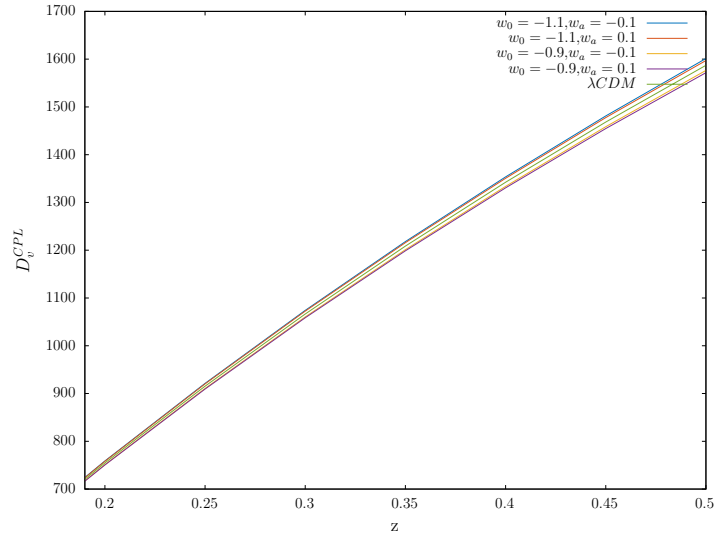

Figure 6.3: The dilation parameter D_V for the different CPL parametrizations.

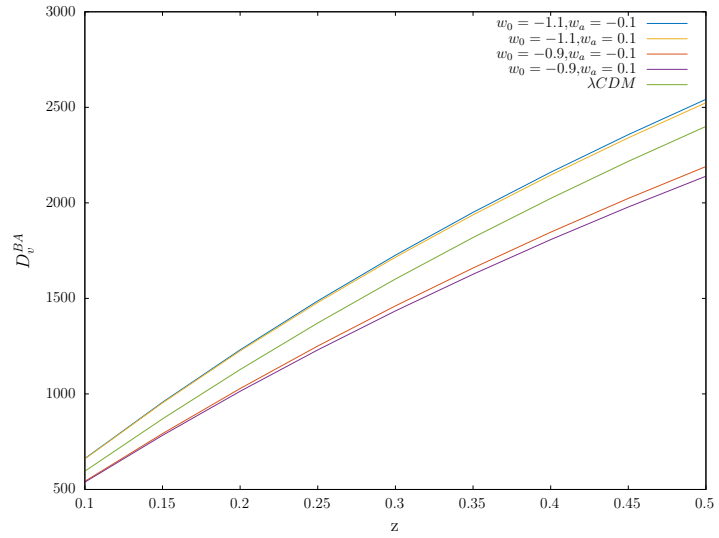

Figure 6.4: The dilation parameter D_V for the different BA parametrizations.

survey, [311] we know that the dilation factor $D_A^{2/3}\, H^{-1/3}$ shall be measured from

the Lyman-α data at an accuracy level of 1.9% at $z \sim 2.5$. Here we investigate the possibility of improving the accuracy of the distance estimates by measuring the cross-correlation of the BOSS Lyman-α data with redshifted 21-cm maps, to the extent that models other than the $LCDM$ may be constrained. We propose a radio interferometric observation of the 21-cm signal with a SKA-1-Mid like telescope and a BOSS like quasar survey to investigate the possibility of constraining dynamical dark energy models.

The Baryon acoustic oscillation (BAO) observations [313] has the potential to constrain the angular diameter distance $d_A(z)$ and the Hubble parameter $H(z)$ through the imprint of the oscillatory feature of the matter power spectrum in the transverse (angular) and longitudinal directions respectively. However, due to low SNR, it is often useful to measure an effective distance defined as [275]

$$D_V(z) = \left[(1+z)^2 d_A(z)^2 \frac{cz}{H(z)}\right]^{1/3} \tag{6.5}$$

This effective distance is a direct quantifier of the underlysing dark energy model. A dimensionless quantity [314]

$$r_{BAO}(z) = \frac{r_s}{D_V(z)} \tag{6.6}$$

is often used in the context of BAO measurements. Here, r_s denotes the sound horizon at the epoch of recombination. Figure (6.5) shows the effect of dynamical

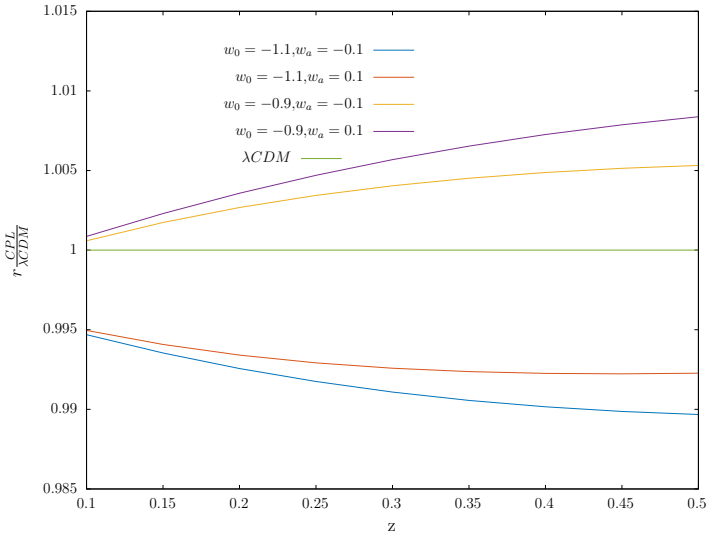

Figure 6.5: The CPL model ratio of r_{BAO} with the LCDM model estimate

dark energy on $r_{_{BAO}}$ as a function of z from the ΛCDM model prediction. A redshift dependent difference of a few percent from the ΛCDM model is seen for the different CPL parametrizations. The behaviour is very similar for the CPL and BA parametrizations which are known to mimic the thawing class of dark energy models.

6.3 The Baryon Acoustic Oscillations

The sound horizon s at the epoch of recombination sets a characteristic length scale which maybe used as a standard ruler. This characteristic scale is given by

$$s = \int_a^{a_{rec}} \frac{c_s(a)}{a^2 H(a)} da \tag{6.7}$$

where a_{rec} denotes the cosmological scale factor at the epoch of recombination. The sound speed c_s is given by $c_s(a) = c/\sqrt{3(1+3\rho_b/4\rho_\gamma)}$, where ρ_b and ρ_γ denotes the photon and baryonic densities respectively.

The comoving length-scale s provides us with a natural standard ruler and defines a transverse angular scale

$$\theta_s = \frac{s}{[(1+z)D_A(z)]}$$

and a radial redshift interval

$$\Delta z_s = \frac{sH(z)}{c}.$$

Here, $D_A(z)$ and $H(z)$ are the angular diameter distance and Hubble parameter at the redshift z respectively. The comoving length-scale $s = 143\,\mathrm{Mpc}$ corresponds to $\theta_s = 1.38^\circ$ and $\Delta z_s = 0.07$ at $z = 2.5$. Measurement of θ_s and Δz_s separately, allows the independent determination of $D_A(z)$ and $H(z)$. Here we consider the determination of these two parameters from the BAO imprint on the cross-correlation signal. We now derive formulas to make error predictions for these parameters.

We start with the Fisher matrix

$$F_{ij} = \sum \frac{1}{\Delta \mathcal{P}_{\mathcal{F}T}^2} \frac{\partial \mathcal{P}_{\mathcal{F}T}}{\partial q_i} \frac{\partial \mathcal{P}_{\mathcal{F}T}}{\partial q_j} \tag{6.8}$$

where q_i refer to the cosmological parameters to be constrained. Here, the cross-

correlation power spectrum is given by

$$\mathcal{P}_{\mathcal{F}T} = C_T C_{\mathcal{F}}(1+\beta_T\mu^2)(1+\beta_{\mathcal{F}}\mu^2)P(k) \tag{6.9}$$

where the various quantities are defined in earlier chapters (see chapter 4)

We then have the Fisher matrix

$$F_{ij} = \frac{V}{(2\pi)^3}\int \frac{d^3\mathbf{k}}{[\mathcal{P}^2_{\mathcal{F}T}(\mathbf{k}) + \mathcal{P}_{\mathcal{F}\mathcal{F}o}(\mathbf{k})\mathcal{P}_{TTo}(\mathbf{k})]}\frac{\partial\mathcal{P}_{\mathcal{F}T}(\mathbf{k})}{\partial q_i}\frac{\partial\mathcal{P}_{\mathcal{F}T}(\mathbf{k})}{\partial q_j} \tag{6.10}$$

The quantities $\mathcal{P}_{TTo}(\mathbf{k})$ and $\mathcal{P}_{\mathcal{F}\mathcal{F}o}(\mathbf{k})$ denote the auto-correlation power spectrum of 21-cm and Lyman-α forest where we include the corresponding observational noises as in Chapter-4. In this work we would like to isolate the BAO imprint and ignore everything else. This BAO information is pn large scales (small wave numbers) with the first peak at roughly $k \sim 0.045\text{Mpc}^{-1}$. The subsequent wiggles are well suppressed by $k \sim 0.3\text{Mpc}^{-1}$. Thus we ignore the limits of the integral in eq. (6.10) and consider an integral over the entire $\mathbf{k}$ space.

The subsequent analysis closely follows [315] and we use $P_b = P - P_c$ to isolate the baryonic features in the power spectrum, and we use this in the derivative $\partial P(k)/\partial q_i$. Here P_c refers to the CDM power spectrum without any baryonic effects. Thus we may write

$$P_b(\mathbf{k}) = \sqrt{8\pi^2}A\,\frac{\sin x}{x}\,\exp\left[-\left(\frac{k}{k_{silk}}\right)^{1.4}\right]\exp\left[-\left(\frac{k^2}{2k_{nl}^2}\right)\right] \tag{6.11}$$

where k_{silk} and k_{nl} denotes the scale of 'Silk-damping' and the scale of 'non-linearity' respectively. In our analysis we take we have used $k_{nl} = (3.07\,h^{-1}\text{Mpc})^{-1}$ and $k_{silk} = (7.76\,h^{-1}\text{Mpc})^{-1}$ from [315]. The constant A is a normalization and we define $x = \sqrt{k_\perp^2 s_\perp^2 + k_\parallel^2 s_\parallel^2}$ where $s_\perp$ and $s_\parallel$ corresponds to θ_s and Δz_s in distance units. The value of s is known accurately from CMBR observations, and the values of $s_\perp$ and $s_\parallel$ are equal to s for the reference values of D_A and $H(z)$. Thus the changes in D_A and $H(z)$ are reflected as changes in the values of $s_\perp$ and $s_\parallel$ respectively, and thus the fractional errors in $s_\perp$ and $s_\parallel$ correspond to fractional errors in D_A and $H(z)$ respectively. We choose $q_1 = \ln(s_\perp^{-1})$ and $q_2 = \ln(s_\parallel)$ as unknown parameters in our analysis, and determine the precision at which it will be possible to constrain these using the location of the BAO features in the cross-correlation

signal. Following [315] we have the $2-D$ Fisher matrix

$$F_{ij} = VA^2 \int dk \int_{-1}^{1} d\mu \frac{k^2 \exp[-2(k/k_{silk})^{1.4} - (k/k_{nl})^2]}{[P^2(k) + \mathcal{P}_{\mathcal{F}\mathcal{F}o}(\mathbf{k})\mathcal{P}_{TTo}(\mathbf{k})/F^2_{\mathcal{F}T}(\mu)]} f_i(\mu) f_j(\mu) \tag{6.12}$$

where $f_1 = \mu^2 - 1$ and $f_2 = \mu^2$ and

$$F^2_{\mathcal{F}T} = (1 + \beta_{\mathcal{F}}\mu^2)(1 + \beta_T \mu^2)$$

The Cramer-Rao bound $\delta q_i = \sqrt{F_{ii}^{-1}}$ is used to calculate the error in the parameter q_i. The error in the combined distance measure D_V, also referred to as the "dilation factor" [316] $D_V(z)^3 = (1+z)^2 D_A(z)\frac{cz}{H(z)}$ (this is often used as a single parameter to quantify BAO observations) is given by

$$\frac{\delta D_V}{D_V} = \frac{1}{3}(4F_{11}^{-1} + 4F_{12}^{-1} + F_{22}^{-1})^{0.5} \tag{6.13}$$

to calculate the relative error in D_V. This quantity is useful when the sensitivity of the individual measurements of D_A and $H(z)$ is low.

6.4 Results

For the error estimation we follow the Fisher matrix analysis as used in the earlier chapter (see Chapter-4). We consider a radio-interferometeric observation with

Table 6.1: Telescope specifications

Observation time T (hrs)	Freq. range(MHz)	T_{sys}(K)	N_{ant}	ΔU	$A_{eff}(m^2)$
400	350-450	60	250	32	150

a SKA-1 mid type of interferometer with a central observing frequency of $\nu =$ 405MHz and a bandwidth of 100MHz. We consider 500 dishes with 15m diameter each with 80% of the antennas in a central core region of radium 1 Km. We have considered 50 independent pointings of 400 hrs observation in each pointing. This uses the BOSS data covering a dominant portion of the sky. For the Lyman-α survey we consider a BOSS like survey with quasar number density of $\bar{n}_Q = 64 deg^{-2}$. We have assumed that the Lyman-α spectrum is measured for each quasar at a SNR of $5-\sigma$.

The BAO imprint on the cross-power spectrum, is used in the Fisher matrix

to constrain $\delta H/H$ and $\delta d_A/d_A$ around the fiducial LCDM model for the CPL and BA parametrizations. The Fisher matrix is also marginalized over the overall normalization in the power spectrum which has modelling uncertainties. The errors in H and d_A are then used to make error projections on the parameters (w_0, w_a) . This is obtained through a transformation of the Fisher matrix as

$$F(w_0, w_a)_{ij} = \sum_m \sum_n \mathcal{M}^T_{im}\ F(H, d_A)_{mn}\ \mathcal{M}_{nj} \tag{6.14}$$

where $F(w_0, w_a)$ is the Fisher matrix for the parameters (w_0, w_a) and $F(H(z_{fid}, d_A(z_{fid}))$ is the Fisher matrix for the parameters $H(z)$ and $D_A(z)$. The transformation matrix is given by

$$\mathcal{M}_{mn}(z_{fid}) = \frac{\partial \xi_m}{\partial \rho_n} \tag{6.15}$$

where $(\xi_m = H(z),\ D_A(z))$ and $(\rho_n = w_0,\ w_a)$

At a fiducial $z_{fid} = 2.5$ and for CPL model with LCDM fiducial values for (w_0, w_a), the Fisher matrix analysis yields the following $1-\sigma$ errors

$$CPL: \quad (\delta D_V/D_V, \delta d_A/d_A, \delta H/H) = (0.42, 0.48, 0.51)\,\% \tag{6.16}$$

The corresponding errors for the BA model are

$$BA: \quad (\delta D_V/D_V, \delta d_A/d_A, \delta H/H) = (0.38, 0.46, 0.48)\,\% \tag{6.17}$$

The projected 1-σ errors on (w_0, w_a) is summarized in the following table.

SKA1-Mid $\times BOSS$		
CPL Model	$\Delta w_0 = 0.089$	$\Delta w_a = 0.245$
BA Model	$\Delta w_0 = 0.084$	$\Delta w_a = 0.165$

Table 6.2: The $1-\sigma$ errors on (w_0, w_a) from BAO imprint on the cross-correlation power spectrum.

We find that the BA model provides tighter constraints on the dynamics of dark energy as compared to the traditionaly used CPL parametrization.

The error projections for the parameters (w_0, w_a) for CPL model has been studied for the eBOSS and DESI. The limits of the error contours and the results are similar to our projections at $z = 2.5$. The PLANCK+DESI data constrains for (w_0, w_a) are $w_0 = (-1.13, -0.86)$ and $w_a = (-0.4, 0.4)$, which also has comparable

figure of merit. Thus, we note that the BAO imprint on the cross-correlations between the HI-21cm signal and Ly-α forest provides competitive constrains in the (w_0, w_a) parameter space at high redshifts.

We conclude by noting that the imprint of the BAO feature on the cross-correlation power spectrum of the HI 21-cm signal and the Lyman-α forest from the post reionization epoch is a direct probe of cosmological structure formation. This signal can be detected with a high SNR with the sensitivity projected for upcoming QSO surveys and 21-cm observations. The cross-correlation has the usual advantages over the individual auto correlations and we find that dynamic dark energy with model-independent parametrizations may be constrained using this probe. Further, improved constraints can be obtained when cross-correlation signal is also combined with other cosmological probes like CMB, BAO, SNIa etc for a joint analysis.